CHEMISTRY
A EUROPEAN JOURNAL

DOI: 10.1002/chem.200800765

Probing Kinase Activities by Electrochemistry, Contact-Angle Measurements, and Molecular-Force Interactions

Ofer I. Wilner, Claudio Guidotti, Agnieszka Wieckowska, Ron Gill, and Itamar Willner*[a]

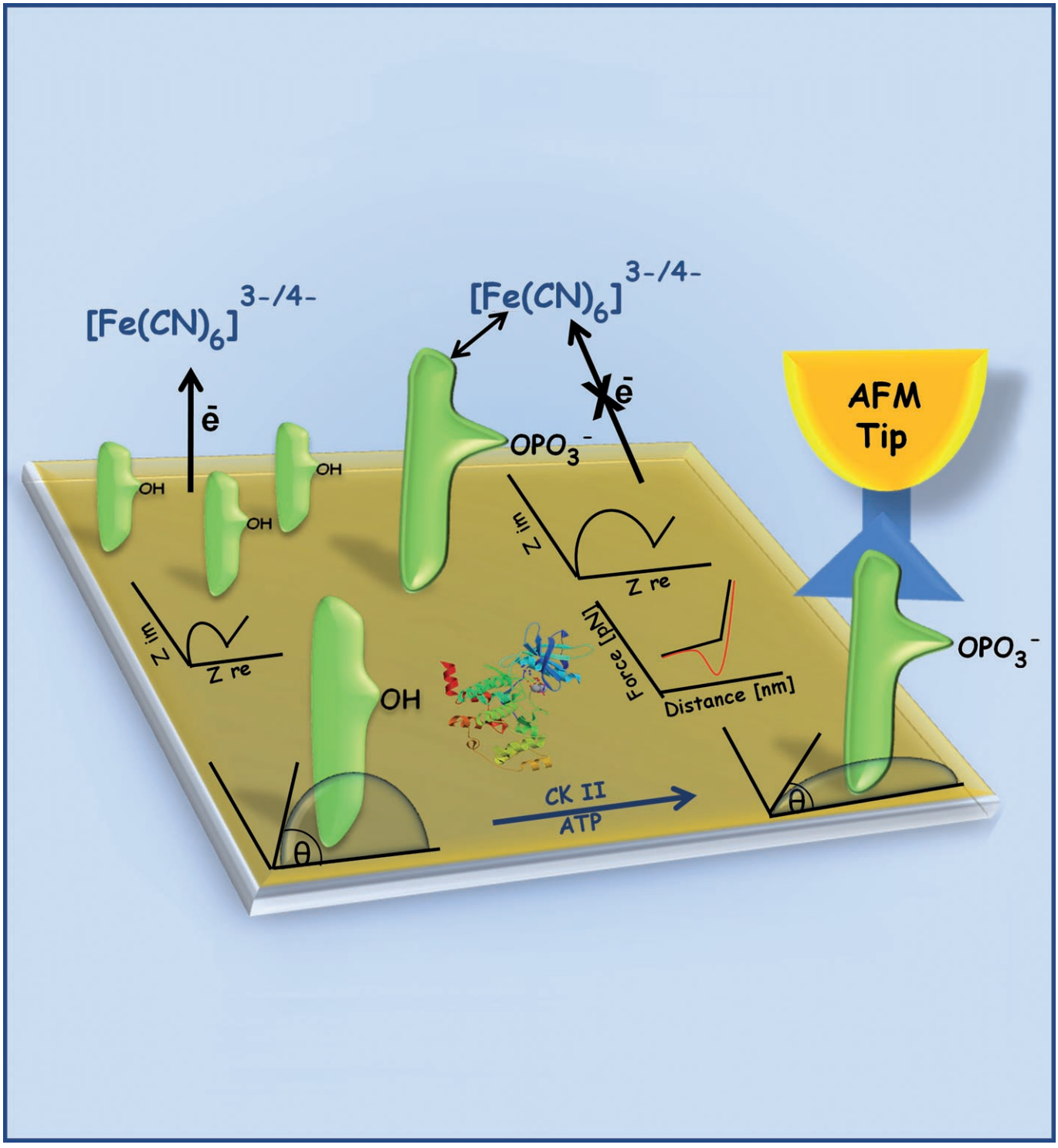

Abstract: Three different methods to investigate the activity of a protein kinase (casein kinase, CK2) are described. The phosphorylation of the sequence-specific peptide (**1**) by CK2 was monitored by electrochemical impedance spectroscopy (EIS). Phosphorylation of the peptide monolayer assembled on a Au electrode yields a negatively charged surface that electrostatically repels the negatively charged redox label $[Fe(CN)_6]^{3-/4-}$, thus increasing the interfacial electron-transfer resistance. The phosphorylation process by CK2 is further amplified by the association of the anti-phosphorylated peptide antibody to the monolayer. Binding of the antibody insulates the electrode surface, thus increasing the interfacial electron-transfer resistance in the presence of the redox label. This method enabled the quantitative analysis of the concentration of CK2 with a detection limit of ten units. The second method employed involved contact-angle measurements. Although the peptide **1**-functionalized electrode revealed a contact angle of 67.5°, phosphorylation of the peptide yielded a surface with enhanced hydrophilicity, 36.8°. The biocatalyzed cleavage of the phosphate units with alkaline phosphatase regenerates the hydrophobic peptide monolayer, contact angle 55.3°. The third method to characterize the CK2 system involved chemical force measurements between the phosphorylated peptide monolayer associated with the Au surface and a Au tip functionalized with the anti-phosphorylated peptide antibody. Although no significant rupture forces existed between the modified tip and the **1**-functionalized surface (6 ± 2 pN), significant rupture forces (multiples of 120 ± 20 pN) were observed between the phosphorylated monolayer-modified surface and the antibody-functionalized tip. This rupture force is attributed to the dissociation of a simple binding event between the phosphorylated peptide and the fluorescent antibody (Fab) binding region.

Keywords: antibodies · biosensors · contact angles · electrochemistry · protein kinases

Introduction

The phosphorylation of proteins by protein kinase is a key process in signal transduction and the regulation of intracellular processes.[1]The over-expression of protein kinases has been reported to be involved in different diseases, such as cancer[2] or Alzheimer's disease.[3] Hence, the rapid detection of the activity of protein kinases is of immediate significance for clinical diagnostics. Different methods for the detection of protein kinases have been developed, such as immunoassays that use fluorescence-labeled antibodies (Fab) against sequence-specific phosphorylated peptides,[4] and the protein kinase-induced radioactive labeling of the phosphorylated product with radioactive ATP.[5] Other methods to monitor the activities of protein kinases include the fluorescence polarization assay,[6] the amplified electrochemical detection of kinase with Au nanoparticles,[7] a protein kinase-induced aggregation of Au nanoparticles,[8] and detection of the depletion of ATP as a result of a biocatalyzed phosphorylation process.[9] Furthermore, a label-free detection of protein kinase was achieved by monitoring the phosphorylation reaction on a field-effect transistor device.[10] In the present study, we probed the activity of casein kinase, CK2, which phosphorylates serine/threonine residues of proteins. At least 160 different proteins are phosphorylated by CK2, and many of these proteins are active in intracellular signal transduction, DNA replication, the synthesis of proteins, and cell division and proliferation. The CK2 is localized in the nuclei of the cells and exists also in the cytosol.[11] The enzyme is a heterotetramer composed of α, α′ and β subunits. The α and α′ subunits are catalytically active and the β subunits recognize the substrates and synergistically stimulate the catalytic activity of the α/α′ subunits.[12]

Here, we introduced different methods to monitor the activities of kinases (specifically, casein kinase), namely, electrochemical impedance spectroscopy, contact angle, and chemical force measurements.

Results and Discussion

Electrochemical impedance spectroscopy is a versatile tool to follow biocatalytic reactions and biomolecular recognition events at electrode surfaces.[13] The electron-transfer resistances at modified electrodes, in the presence of a redox label solubilized in the bulk electrolyte solution, are strongly dependent on electrostatic interactions between the redox label in the electrolyte solution and the charged electrode surface or changes in the dielectric properties of the surface caused by the biocatalytic or biorecognition events.[14] For example, DNA hybridization on electrode surfaces was analyzed in the presence of $[Fe(CN)_6]^{3-/4-}$ as redox label by means of electrochemical impedance spectroscopy (EIS). The hybridization of the analyte DNA with the capturing nucleic acid linked to the electrode increased the interfacial electron-transfer resistances as a result of the electrostatic repulsion of the redox label.[15] Similarly, EIS was applied to follow the formation of an aptamer–adenosine complex by

[a] O. I. Wilner, Dr. C. Guidotti, Dr. A. Wieckowska, R. Gill, Prof. Dr. I. Willner
Institute of Chemistry, The Hebrew University of Jerusalem
Jerusalem 91904 (Israel)
Fax: (+972) 2-652-7715
E-mail: willnea@vms.huji.ac.il

Supporting information for this article is available on the WWW under http://dx.doi.org/10.1002/chem.200800765.

the separation of an aptamer–nucleic acid duplex associated with the electrode, and the subsequent decrease of the interfacial electron-transfer resistances.[16] The association of proteins to electrode surfaces insulates these surfaces and thus increases the interfacial electron-transfer resistances in the presence of a solubilized redox label. This has been used to detect the association of proteins to electrodes and, specifically, to monitor the formation of immunocomplexes on electrodes,[17] and to develop EIS-based immunosensors. Furthermore, biocatalytic transformations at electrode surfaces, such as enzyme cleavage of duplex DNA[18] or the biocatalytic deposition of insoluble products on electrodes[19] were investigated by EIS.

In the present study, EIS measurements were applied to measure casein kinase (CK2) activity by probing the interfacial electron-transfer resistances, R_{et}, in the presence of $[Fe(CN)_6]^{3-/4-}$ as redox label (Scheme 1). Electrostatic interactions between the interface and charged redox labels in solution are known to control the interfacial electron-transfer resistances.[13,15,18] Specifically, a surface that becomes negatively charged as a result of a chemical transformation will be accompanied by an increase in the electron-transfer resistance in the presence of a negatively charged redox label in the electrolyte solution (due to the repulsion of the label), and a decrease in the interfacial electron-transfer resistance in the presence of a positively charged redox label (due to electrostatic attraction of the label).[20] In the present system, the phosphorylation of the peptide monolayer produces a negatively charged peptide, and hence, an increase in the electron-transfer resistance is anticipated upon using the negatively charged redox label $[Fe(CN)_6]^{3-/4-}$. It should be noted, however, that the peptide carries seven carboxylic acid residues as opposed to two positive arginine units, and thus, the peptide is negatively charged already prior to the phosphorylation. As a positively charged redox label ($Ru(NH_3)_6^{3+}$) is attracted to the surface prior to phosphorylation and yields a $R_{et} \approx 0$, a positively charged label cannot be used in the present study to probe the phosphorylation reaction.

Peptide **1** is the substrate of CK2. This peptide was immobilized on an electrode surface by the primary modification of the electrode with the thiolated *N*-hydroxysuccinimide active ester monolayer, followed by coupling of **1** to the surface. The surface coverage of **1** on the Au surface was estimated by microgravimetric quartz crystal microbalance (QCM) measurements to be 3.3×10^{-11} mole cm^{-2}. The CK2-catalyzed phosphorylation of the serine residue in **1** yields the phosphorylated product **2**. The negative charges resulting on the surface electrostatically repel the negatively charged redox label, and hence, the interfacial electron-transfer resistance increase as expected. The association of the antibody that is specific for the CK2 product **2** is antici-

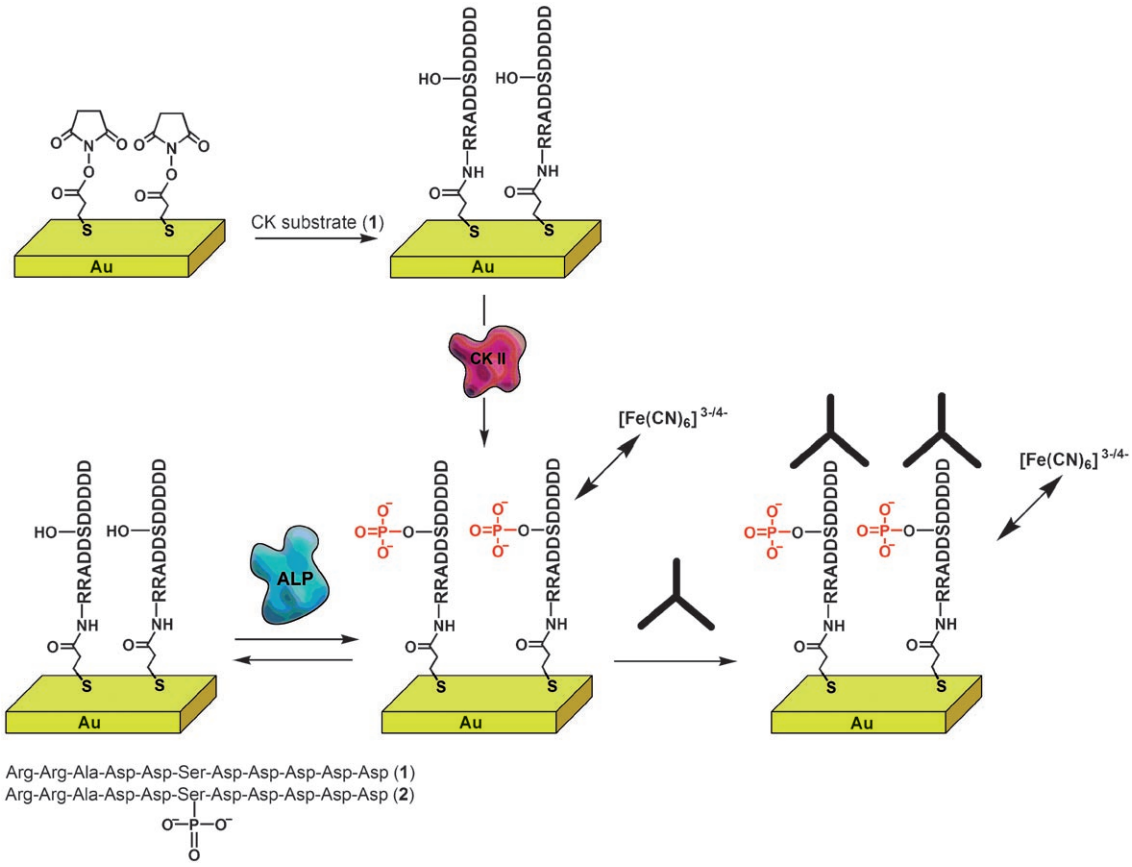

Scheme 1. Analysis and amplification of casein kinase activity by electrochemical impedance spectroscopy (ALP = alkaline phosphatase).

pated to further block the electron transfer and thus increase the interfacial electron-transfer resistance. Figure 1A shows the time-dependent electrochemical impedance spectra (in the form of Nyquist plots) of the **1**-modified Au electrode upon treatment with CK2 (500 U). The interfacial

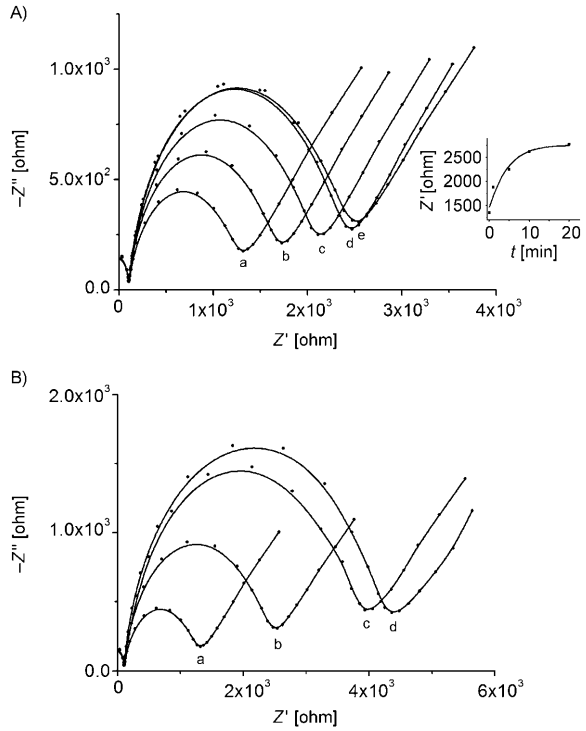

Figure 1. A) Time-dependent electrochemical impedance spectra (in the form of Nyquist plots) showing phosphorylation of the **1**-functionalized electrode by CK2 (500 U) and ATP (0.1 mM) for different time intervals: a) 0, b) 1, c) 5, d) 10, e) 20 min. Inset: time-dependent changes of the interfacial electron-transfer resistances upon phosphorylation of the **1**-modified electrode. B) Electrochemical impedance spectra for a) the **1**-modified Au electrode, b) after phosphorylation of the monolayer with CK2 (500 U) and ATP (0.1 mM) for 20 min, c) and d) after the treatment of the phosphorylated monolayer with the anti-phosphorylated peptide Ab (1 $\mu g\,mL^{-1}$) for 10 and 20 min, respectively. All experiments were performed in HEPES buffer (0.05 M, pH 7.4) using $[Fe(CN)_6]^{3-/4-}$ as redox label. A bias potential of 0.2 V vs SCE was applied, and a 10-mV alternate voltage in a frequency range of 100 MHz–10 kHz was used.

electron-transfer resistances increase as the biocatalytic process is prolonged, and the interfacial electron-transfer resistance reaches a saturation value of $R_{et}=2.7$ kΩ after approximately 20 min of reaction (Figure 1A, inset). This is consistent with the fact that increasing the time interval of the biocatalytic reaction enhances the negative charge associated with the surface, resulting in progressively higher interfacial electron-transfer resistances. Saturation of the impedance spectra implies either complete phosphorylation of the monolayer or the equilibrium state, in which the negatively charged ATP is electrostatically repelled from the phosphorylated monolayer, thus blocking further phosphorylation. Control experiments revealed that the impedance spectrum of the **1**-functionalized Au electrode did not change upon treatment of the surface with CK2 or ATP only. Furthermore, treatment of the electrode modified with the phosphorylated monolayers with alkaline phosphatase removed the phosphate groups and restored the spectrum of the **1**-modified surface. These results demonstrate that the biocatalyzed phosphorylation of the peptide is, indeed, the origin for the changes in the impedance spectra. Figure 1B shows the electrochemical impedance spectra of the **1**-functionalized electrode (a), the phosphorylated monolayer after treatment with CK2 for 20 min (b), and the **2**-modified surface after treatment with the antibody for 10 and 20 min (c) and (d), respectively.

The interfacial electron-transfer resistances (R_{et}) increase upon association of the antibody (Ab) from 2.7 to 4.5 kΩ, consistent with the association of the antibody to the phosphorylated antigen and the blocking effect of the bound protein on the interfacial electron transfer. Figure 2 depicts the quantitative analysis of CK2 by EIS. In this experiment, the **1**-functionalized electrodes were reacted with CK2/ATP for a fixed time interval of ten minutes, and subsequently, the phosphorylated monolayer-modified electrodes were challenged with the anti-**2**-Ab. Figure 2c and e show the Nyquist plots of the phosphorylated surface, generated upon challenging the electrode with CK2 (250 U), before and after treatment with the Ab, respectively. Similarly, curves d and f show the impedance spectra of the **1**-modified electrode treated with CK2 (500 U), before and after reaction with the anti-**2**-Ab, respectively. The interfacial electron-transfer

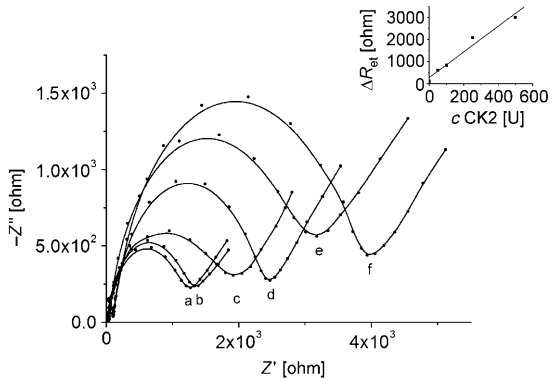

Figure 2. Electrochemical impedance spectra showing analysis of different concentrations of CK2, according to Scheme 1: a) the **1**-functionalized electrode, b) the **1**-functionalized electrode treated for 10 min with the anti-phosphorylated peptide antibody, c) the phosphorylated peptide monolayer generated by 250 U of CK2 for 20 min, d) the phosphorylated peptide monolayer generated by 500 U of CK2 for 20 min, e) the phosphorylated monolayer generated in (c) after treatment with the anti-phosphoserine antibody (1 $\mu g\,mL^{-1}$) for 10 min, f) the phosphorylated monolayer generated in (d) after treatment with the antibody (1 $\mu g\,mL^{-1}$) for 10 min. Inset: calibration curve showing changes in the interfacial electron-transfer resistances upon analyzing different concentrations of CK2 by the antibody-amplified scheme (ΔR_{et} represents the difference between the electron-transfer resistance after the association of the antibody to the phosphorylated monolayer and the electron-transfer resistance at the **1**-functionalized electrode). All experiments were performed in 0.05 M HEPES buffer, pH 7.4, using $[Fe(CN)_6]^{3-/4-}$ as redox label. A bias potential of 0.2 V vs. SCE was applied, and a 10-mV alternate voltage in a frequency range of 100 MHz–10 kHz was used.

resistances of the two electrodes after phosphorylation have values of 1.9 and 2.5 kΩ, respectively, and after association of antibodies the interfacial electron-transfer resistances increase to 3.4 and 4.3 kΩ, respectively. The extent of phosphorylation of the **1**-modified peptide monolayer is controlled by the concentration of CK2. Hence, the increase in the interfacial electron-transfer resistance is controlled by the concentration of CK2, and the electron-transfer resistances increase as the concentration of CK2 is elevated. For example, increasing the concentration of CK2 from 250 to 500 U induces changes in the interfacial electron-transfer resistances of 600 and 900 Ω, respectively (Figure 2c and d, respectively). These interfacial changes are, however, less accurate upon analyzing lower concentrations of CK2 that result in lower coverage of the phosphorylated product (the reduced accuracy is due mainly to slight differences in the electrode surface area and the coverage of the surface by **1** for different electrodes). The greater differences in the interfacial electron-transfer resistances as a result of association of the Ab to the phosphorylated surface allow us to probe with good accuracy low concentrations of CK2. Figure 2, inset, shows the derived calibration curve. The CK2 could be analyzed with a sensitivity of 10 U.

A series of control experiments demonstrated the specificity of phosphorylation of the **1**-functionalized monolayer electrode by CK2, and revealed the specificity of the **2**-modified electrode towards the anti-**2**-Ab (see Supporting Information). In one set of experiments (Figure S1), the **1**-functionalized monolayer was interacted with the foreign tyrosine kinase (Src kinase) and ATP. Only a minute change in the interfacial electron-transfer resistance, $\Delta R_{et} = 100\ \Omega$, was observed, implying that the foreign kinase does not phosphorylate the peptide. Treatment of the same electrode with CK2 and ATP induced a large change in the interfacial electron-transfer resistance, $\Delta R_{et} = 900\ \Omega$, consistent with the effective phosphorylation of the surface. Treatment of the resulting phosphorylated **2**-monolayer electrode with the foreign anti-BSA Ab resulted in a minute change in the interfacial electron-transfer resistance, $\Delta R_{et} = 70\ \Omega$, indicating that the anti-**2**-Ab binds specifically to the surface. In a set of further control experiments (Figure S2), the specificity of the phosphorylation of peptides by different kinases was examined. In these experiments, the Au electrode was functionalized with the Src-kinase-specific peptide substrate. The CK2 and ATP did not induce any significant change in the interfacial electron-transfer resistance, but treatment of this electrode with the tyrosine kinase (Src kinase) and ATP yielded a ΔR_{et} of approximately 1200 Ω. These results indicate that electrochemical impedance spectroscopy might be used as a versatile method to monitor different kinases.

Control of the hydrophilic/hydrophobic properties of surfaces is a subject of extensive research.[21] Particularly interesting are systems in which the surface properties are reversibly controlled by means of external signals such as electrochemical,[22] photochemical,[23] or chemical[24] stimuli. The use of enzymes to reversibly control surface properties is, however, rare.[25] The phosphorylation of peptides by kinases and the formation of negatively charged products, together with the availability of phosphatases, such as alkaline phosphatase, that cleave off the phosphate groups suggest that surface properties could be interchanged by these two families of enzymes. The formation of a negatively charged peptide monolayer on the Au surface upon the CK2-mediated phosphorylation of **1** is anticipated to yield a surface of enhanced hydrophilicity, whereas the alkaline phosphatase-induced cleavage of the phosphate units is expected to restore the **1**-functionalized surface of enhanced hydrophobicity. Figure 3a shows the shape of an aqueous droplet on the **1**-functionalized surface. The resulting contact angle was 67.5°.

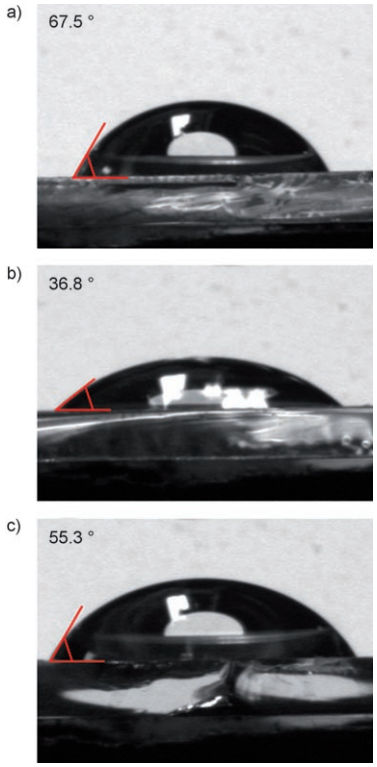

Figure 3. Images of aqueous droplets consisting of 50-mM HEPES buffer on: a) the **1**-functionalized Au surface, b) the phosphorylated peptide monolayer-modified surface, c) the dephosphorylated monolayer after treatment of the **2**-modified electrode with alkaline phosphatase (20 U).

Figure 3b depicts the shape of an aqueous droplet deposited on the **1**-functionalized Au surface after its treatment with CK2/ATP (CK2 = 500 U) and the formation of the phosphorylated surface. Clearly, the aqueous droplet is flattened on the surface, contact angle 36.8°, consistent with the formation of a surface with increased hydrophilicity. The subsequent treatment of the surface with alkaline phosphatase resulted in the dephosphorylation of the peptide to the **1**-modified surface. Figure 3c shows the image of the resulting droplet. The contact angle of the droplet is 55.3°, consistent with regeneration of the **1**-modified surface. Accordingly, the surface could be cycled between hydrophilic and hydrophobic states by means of the two biocatalytic transforma-

tions. Control experiments revealed that treatment of the **1**-modified surface with either CK2 or ATP alone did not affect the contact angle of the **1**-modified surface. This implies that the phosphorylation and dephosphorylation processes are, indeed, responsible for the observed changes in the contact angles. The biocatalytic control over the hydrophilicity of the surface is attributed to the fact that phosphorylation of the serine unit in the **1**-modified surface yields an anionic site that enhances the hydrophilic nature of the monolayer-modified surface. The dephosphorylation of the phosphate group by phosphatase regenerated the serine unit, resulting in a surface of hydrophobicity comparable to the original **1**-modified surface.

The characterization of biomolecular interactions by means of chemical-force measurements has been addressed in numerous studies.[26] For example, DNA hybridization,[27] antigen–antibody complex formation,[28] aptamer–protein interactions,[29] or biotin–avidin binding[30] were characterized by means of chemical-force microscopy. The analysis of biocatalytic transformations by means of chemical force microscopy is, however, rare, and only a few examples have been reported.[24,31] For example, the activity of tyrosinase was analyzed by force microscopy, by detecting the enzyme-stimulated generation of cathechol units on surfaces by means of force interactions exerted through π-donor–acceptor interactions between a π-acceptor-modified tip and the π-donor cathechol-functionalized surface. The availability of the specific antibody for the phosphorylated peptide (**2**) formed by CK2 suggests that force interactions could be applied to monitor the enzyme activity through the separation of the respective immunocomplex. Accordingly, a Au surface was modified with the peptide **1**, and a Au-coated AFM tip was functionalized with the antibody against the phosphorylated **2** (Figure 4A). The **1**-modified surface was subjected to CK2/ATP and the force interactions between the antibody-functionalized tip and the modified surface were monitored before and after the reaction with CK2/ATP. Subsequently, the phosphorylated **2**-modified surface was reacted with alkaline phosphatase, and the force interactions between the antibody-functionalized tip and the surface were characterized. Figure 4B shows representative force curves between the Ab-modified tip and the **1**-functionalized surface (a), after phosphorylation (b), and after treatment of the phosphorylated surface with phosphatase (c). Figure 4C shows histograms of the forces between the Ab-modified tip and the **1**-functionalized surface (a), forces between the Ab-functionalized tip and the phosphorylated surface (b), and the forces between the Ab-modified tip with **1**-functionalized surface after treatment with phosphatase (c). The average force between the **1**-modified surface and the functionalized tip is 6 pN.

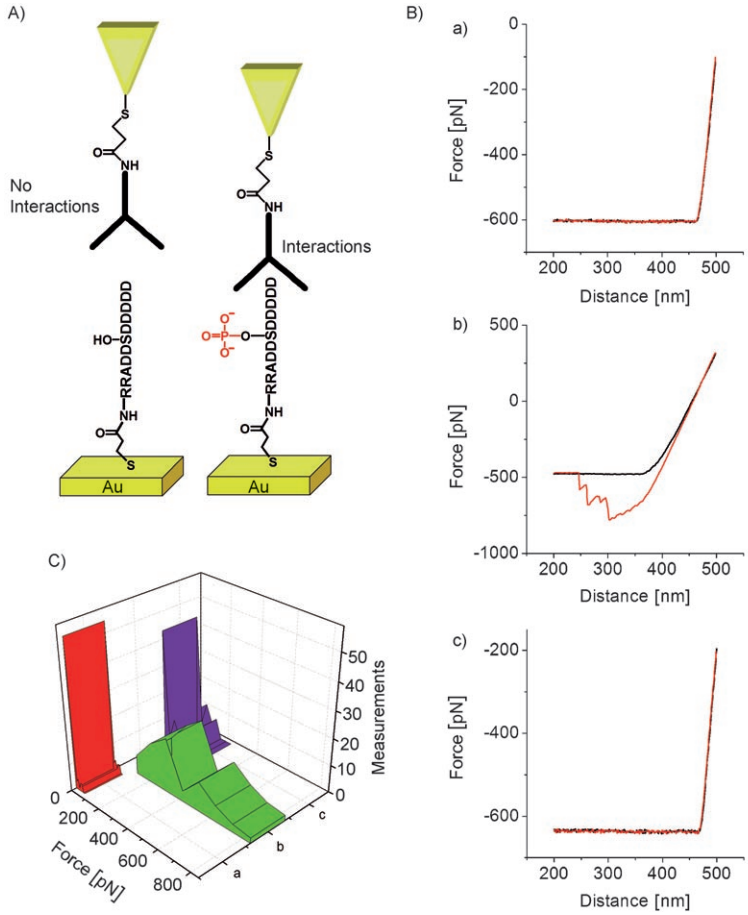

Figure 4. A) Scheme for probing the phosphorylation of the **1**-functionalized surface by CK2/ATP using chemical force microscopy. B) Typical force curves representing interactions of the anti-phosphoserine antibody-modified tip with: a) the **1**-functionalized surface, b) the phosphorylated, **2**-functionalized surface, c) the phosphorylated surface that was treated with alkaline phosphatase to restore the **1**-modified surface. C) Histograms of forces resulting from interactions of the antibody-modified tip with: a) the **1**-functionalized surface, b) the phosphorylated, **2**-modified surface, c) the dephosphorylated monolayer surface generated by treatment of the **2**-modified surface with alkaline phosphatase.

After phosphorylation, substantially higher rupture forces are observed, consistent with the formation of an antibody-phosphorylated peptide on the surface. The observed rupture forces are multiples of 120 ± 10 pN, as rupture forces of 120 ± 10, 240 ± 20, 360 ± 40, up to 960 ± 80 pN were obtained. The basic value of 120 pN is attributed to the rupture forces between the phosphorylated antigen and one of the Fab antibody domains. Indeed, this observed rupture force

value is in the range of rupture forces of other antigen–antibody immunocomplexes originating from a single Fab domain.[32] Treatment of the phosphorylated surface with alkaline phosphatase resulted in a surface that revealed very low rupture forces with the antibody-modified tip, 35 ± 4 pN. This is consistent with alkaline phosphatase removing the phosphate sites, hence depleting the affinity for interaction between the tip and the surface.

In conclusion, the present study has introduced three different methods to probe the biocatalytic activity of CK2 on the **1**-functionalized surface. Electrochemical impedance spectroscopy may be used as quantitative method to analyze the activity of the kinase and to follow the phosphorylation process by amplification of the phosphorylated product through the generation of the respective antigen–antibody complex. Chemical force microscopy enabled us to characterize the specific molecular interactions between the phosphorylated product and the antibody, and contact-angle measurements allowed us to monitor the biocatalytic performance of the kinase by probing the hydrophilicity of the phosphorylated/dephosphorylated peptide-modified surface. We applied these methods to analyze "pure" kinase samples, however, a future goal is their application to actual biological samples.

Experimental Section

All chemicals were purchased from Aldrich and used without further purification. Ultrapure water from a NANOpure Diamond (Barnstead) source was used throughout all experiments. Casein kinase 2 was purchased from New England BioLabs. The substrate of the enzyme (**1**), adenosine triphosphate (ATP), monoclonal anti-phosphoserine antibody, and alkaline phosphatase (E.C. 3.1.3.1) were purchased from Sigma. Tyrosine kinase-Src kinase was purchased from Cell Signaling Technologies. The Src kinase substrate was synthesized by Biosight, Israel.

Modification of electrodes: Au-coated (50 nm Au layer) glass plates (22×22 mm^2) (Analytical μ-Systems, Germany) were sonicated with acetone and isopropanol for 30 min and then washed with ultrapure water. The slides were then dried under a nitrogen stream and immersed for 20 min in a solution of 2 mg of dithio-diNHS (di(*N*-succinimidyl)-3,3′-dithiodipropionate) in 1 mL of DMSO. After multiple rinsing cycles with DMSO and subsequent rinsing with HEPES buffer (0.05 M, pH 7.4) the slides were introduced into a solution of CK2 substrate (peptide **1**, 0.01 μg) in HEPES buffer (0.05 M, pH 7.4) for 1 h in the presence of 0.1 mM of ATP. After rinsing the surfaces with HEPES buffer (0.05 M) the slides were modified with a mercaptohexanol solution (1 mM) for 30 sec to fill any pinhole defects, and to prevent nonspecific adsorption. The resulting modified slides were then reacted with different concentrations of CK2 in Tris buffer, supplied with the enzyme (20 mM, pH 7.5), that included KCl (50 mM) and $MgCl_2$ (10 mM). One unit of enzyme (U) is the amount of enzyme that transfers 1 pmole of phosphate to peptide **1** (100 μM) in one minute at 30°C in a reaction volume of 25 μL. Alkaline phosphatase (ALP) was treated in borate buffer (pH 9.3) and $MgCl_2$ (1 mM).

Electrochemical surface characterization and contact-angle measurements: Electrochemical impedance spectroscopy (EIS) measurements on the modified electrodes were performed using an Autolab electrochemical analyzer (EcoChemie, The Netherlands) connected to a PC (FRA version 4.9 software). Samples were in a $[Fe(CN)_6]^{3-/4-}$ solution (5 mM) in HEPES buffer (0.05 M) with a graphite counter-electrode and a saturated calomel reference electrode (SCE). The electrochemical impedance spectra were recorded by applying a bias potential of 0.2 V vs. SCE, and applying a 5-mV alternate voltage, using 30 equally spaced frequencies, in the frequency range of 100 mHz–10 kHz as perturbation voltage. Electrochemical impedance spectra were plotted as Nyquist diagrams in the form of complex plane diagrams (real impedance Z' plotted vs complex impedance Z''). The experimental impedance spectra were fitted by using electric equivalent circuits. For this purpose commercial software (Zview, version 2.1b, Scribner Associates, Inc.) was employed.

Static contact-angle measurements were performed on the modified Au by using a CAM 2000 Optical-Angle Analyzer (KSV Instruments, Finland). A droplet of the 0.05-M HEPES buffer solution, approximately 20-μL with diameter of roughly 0.5 cm, was deposited on the surface by using a syringe. The images of the droplets were recorded and each contact-angle measurement was repeated at least three times. The reported value represents the average of these results.

AFM: Au-coated AFM cantilevers (Csc 38 Cr–Au MikroMasch) were treated with acetone and isopropanol for 30 min and then washed with ultrapure water. The cantilevers were then immersed for 20 min in a solution of 2 mg of dithio-diNHS (di(*N*-succinimidyl)-3,3′-dithiodipropionate) in 1 mL of DMSO. After multiple rinsing cycles with DMSO and subsequent rinsing with HEPES buffer (0.05 M, pH 7.4), the cantilevers were introduced into a solution of 0.01 μg of anti-phosphoserine Ab (Sigma) in HEPES buffer (0.05 M, pH 7.4) for 1 h.

Force measurements were carried out at RT by using a Multimode scanning probe microscope with a Nanoscope 3A controller and a Pico Force module (Digital Instruments, Veeco Probes, Santa Barbara, CA). The spring constants of the Au-coated cantilevers (MikroMasch, Germany) were determined in air by using the thermal-noise method to give an average spring constant of 0.012 N m^{-1}. All experiments were conducted in the Tris buffer/kinase solution or the alkaline phosphatase/borate buffer in a liquid cell. To measure the force interactions, the probe tip was lowered to the surface and immediately retracted at a rate of 0.1 μm s^{-1}, and data points were analyzed with their associated spring constants. Histograms were prepared by using Origin software. Each histogram was the result of at least 70 separate force measurements.

Acknowledgement

This research was supported by the Israel Science Foundation within the Converging Technologies Program.

[1] G. Manning, D. B. Whyte, R. Martinez, T. Hunter, S. Sudarsanam, *Science* **2002**, *298*, 1912–1934.
[2] P. Cohen, *Nat. Rev. Drug Discovery* **2002**, *6*, 481–490.
[3] a) M. Flajolet, G. He, M. Heiman, A. Lin, A. C. Narin, P. Greengard, *Proc. Natl. Acad. Sci. USA* **2007**, *104*, 4159–4164; b) D. P. Hanger, H. L. Byers, S. Wray, K.-Y. Leung, M. J. Saxton, A. Seereeam, C. H. Reynolds, M. A. Ward, B. H. Anderton, *J. Biol. Chem.* **2007**, *282*, 23645–23654.
[4] J. H. Till, R. S. Annan, S. A. Carr, W. T. Miller, *J. Biol. Chem.* **1994**, *269*, 7423–7428.
[5] C. Lehel, S. Daniel-Issakani, M. Brasseur, B. Strulovici, *Anal. Biochem.* **1997**, *244*, 340–346.
[6] a) A. Flower, D. Swift, E. Longman, A. Acornley, P. Hemsley, D. Murray, J. Unitt, I. Dale, E. Sullivan, M. Coldwell, *Anal. Biochem.* **2002**, *308*, 223–231; b) T. C. Turek-Etienne, M. Lei, J. S. Terracciano, E. F. Langsdorf, R. W. Bryant, R. F. Hart, A. C. Horan, *J. Biomol. Screening* **2004**, *9*, 53–61.
[7] K. Kerman, H.-B. Kraatz, *Chem. Commun.* **2007**, 519–521.
[8] J. Oishi, Y. Asami, T. Mori, J.-H. Kang, M. Tanabe, T. Niidome, Y. Katayama, *ChemBioChem* **2007**, *5*, 875–879.
[9] K. Kupcho, R. Somberg, B. Bulleit, S. A. Goueli, *Anal. Biochem.* **2003**, *317*, 210–217.
[10] R. Freeman, R. Gill, I. Willner, *Chem. Commun.* **2007**, 3450–3452.

[11] a) B. Guerra, O.-G. Issinger, *Electrophoresis* **1999**, *20*, 391–408; b) L. A. Pinna, *Biochim. Biophys. Acta* **1990**, *1054*, 267–284; c) J. E. Allende, C. C. Allende, *FASEB J.* **1995**, *9*, 313–323.
[12] O.-G. Issinger, *Pharmacol. Ther.* **1993**, *59*, 1–30.
[13] E. Katz, I. Willner, *Electroanalysis* **2003**, *15*, 913–947.
[14] F. Patolsky, A. Lichtenstein, I. Willner, *Angew. Chem.* **2000**, *112*, 970–973; *Angew. Chem. Int. Ed.* **2000**, *39*, 940–943.
[15] a) F. Patolsky, A. Lichtenstein, I. Willner, *J. Am. Chem. Soc.* **2001**, *123*, 5194–5205; b) T. H. Degefa, J. Kwak, *J. Electroanal. Chem.* **2008**, *612*, 37–41.
[16] M. Zayats, Y. Huang, R. Gill, C.-A. Ma, I. Willner, *J. Am. Chem. Soc.* **2006**, *128*, 13666–13667.
[17] a) A. B. Kharitonov, L. Alfonta, E. Katz, I. Willner, *J. Electroanal. Chem.* **2000**, *487*, 133–141; b) R. Pei, Z. Cheng, E. Wang, X. Yang, *Biosens. Bioelectron.* **2001**, *16*, 355–361.
[18] L. Alfonta, I. Willner, *Chem. Commun.* **2001**, 1492–1493.
[19] F. Patolsky, A. Lichtenstein, I. Willner, *Chem. Eur. J.* **2003**, *9*, 1137–1145.
[20] V. Pardo-Yissar, E. Katz, O. Lioubashevski, I. Willner, *Langmuir* **2001**, *17*, 1110–1118.
[21] Y. Liu, L. Mu, B. Liu, J. Kong, *Chem. Eur. J.* **2005**, *11*, 2622–2631.
[22] a) J. Lahann, S. Mitragotri, T.-N. Tran, H. Kaido, J. Sundaram, I. S. Choi, S. Hoffer, G. A. Somorjai R. Langer, *Science* **2003**, *299*, 371–374; b) X. Wang, A. B. Kharitonov, E. Katz, I. Willner, *Chem. Commun.* **2003**, 1542–1543; c) E. Katz, O. Lioubashevsky, I. Willner, *J. Am. Chem. Soc.* **2004**, *126*, 15520–15532; d) M. Riskin, B. Basnar, V. I. Chegel, E. Katz, I. Willner, F. Shi, X. Zhang, *J. Am. Chem. Soc.* **2006**, *128*, 1253–1260; e) M. Riskin, B. Basnar, E. Katz, I. Willner, *Chem. Eur. J.* **2006**, *12*, 8549–8557.
[23] a) X. Wang, S. Zeevi, A. B. Kharitonov, E. Katz, I. Willner, *Phys. Chem. Chem. Phys.* **2003**, *5*, 4236–4241; b) R. Rosario, D. Gust, A. A. Garcia, M. Hayes, J. L. Taraci, T. Clement, J. W. Dailey, S. T. Picraux, *J. Phys. Chem. B* **2004**, *108*, 12640–12642; c) W. H. Jiang, G. J. Wang, Y. N. He, X. G. Wang, Y. L. An, Y. L. Song, L. Jiang, *Chem. Commun.* **2005**, 3550–3552.
[24] A. Wieckowska, A. B. Braunschweig, I. Willner, *Chem. Commun.* **2007**, 3918–3920.
[25] A. B. Braunschweig, R. Elnathan, I. Willner, *Nano Lett.* **2007**, *7*, 2030–2036.
[26] a) A. Janshoff, M. Neitzert, Y. Oberdörfer, H. Fuchs, *Angew. Chem.* **2000**, *112*, 3346–3374; *Angew. Chem. Int. Ed.* **2000**, *39*, 3212–3237; b) H. Beyer, M. K. Clausen-Schaumann, *Chem. Rev.* **2005**, *105*, 2921–2948.
[27] a) G. U. Lee, L. A. Chrisey, R. J. Colton, *Science* **1994**, *266*, 771–773; b) T. Strunz, K. Oroszlan, R. Schäfer, H. J. Günterodt, *Proc. Natl. Acad. Sci. USA* **1999**, *96*, 11277–11282; c) R. Krautbauer, M. Rief, H. E. Gaub, *Nano Lett.* **2003**, *3*, 493–496.
[28] R. Ros, F. Schwesinger, D. Anselmetti, M. Kubon, R. Schäfer, A. Plueckthun, L. Tiefenauer, *Proc. Natl. Acad. Sci. USA* **1998**, *95*, 7402–7405.
[29] B. Basnar, R. Elnathan, I. Willner, *Anal. Chem.* **2006**, *78*, 3638–3642.
[30] a) V. T. Moy, E.-L. Florin, H. E. Gaub, *Science* **1994**, *266*, 257–259; b) E.-L. Florin, V. T. Moy, H. E. Gaub, *Science* **1994**, *264*, 415–417; c) G. U. Lee, D. A. Kidwell, R. J. Colton, *Langmuir* **1994**, *10*, 354–357.
[31] a) T. Suzuki, Y.-W. Zhang, T. Koyama, D. Y. Sasaki, K. Kurihara, *J. Am. Chem. Soc.* **2006**, *128*, 15209–15214; b) M. Sletmoen, G. Skjåk-Braek, B. T. Stokke, *Carbohydr. Res.* **2005**, *340*, 2782–2795.
[32] a) U. Dammer, M. Hegner, D. Anselmetti, P. Wagner, M. Dreier, W. Huber, H.-J. Güntherodt, *Biophys. J.* **1996**, *70*, 2437–2441; b) S. Allen, X. Chen, M. C. Davies, A. C. Dawkes, J. C. Edwards, C. J. Roberts, J. Sefton, S. J. B. Tendler, P. M. Williams, *Biochemistry* **1997**, *36*, 7457–7463; c) S. Allen, J. Davies, M. C. Davies, A. C. Dawkes, C. J. Roberts, S. J. B. Tendler, P. M. Williams, *Biochem. J.* **1999**, *341*, 173–178.

Received: April 22, 2008
Published online: August 12, 2008

